Effect of Electrode Amplitude on Flow Separation Suppression by Multi-Wavy Plasma Actuator

Y. MARUKAWA[1]*, I. TAKEMOTO[1], Y. NISHIO[2], H. ISHIKAWA[3]

1: Dept. of Mechanical Engineering, Graduate School, Tokyo University of Science, Japan
2: Dept. of Science and Engineering, Seikei University, Japan
3: Dept. of Mechanical Engineering, Tokyo University of Science, Japan

* Correspondent author: ishi@rs.tus.ac.jp

Abstract

Plasma actuators (PA) have attracted attention as a new device for flow separation control. This study, micro PA with an electrode width of millimeter order or less was applied to suppress the flow separation from NACA airfoil. The electrode geometry of the micro PA was sinusoidal electrodes. Jets induced by wavy electrodes collide with each other to form streamwise vortex. Streamwise vortex mixes the momentum inside and outside the boundary layer around the airfoil and suppresses flow separation. We used the damping type (the electrode amplitude decreases in the streamwise direction) and the growing type (the electrode amplitude increases in the streamwise direction) with four rows of wavy electrodes. These PA were attached to the airfoil to verify how the suppression of flow separation differs depending on the streamwise vortex and jet. The results showed that the damping type, which induced streamwise vortex at the leading edge of the airfoil, was more effective on flow separation suppression than the growing type.

Keyword: *micro plasma actuator, flow separation, airfoil, flow control, streamwise vortex*

1. Introduction

Plasma actuators (PA) have recently attracted attention as a new device for flow separation control. PA has a simple structure in which a dielectric is sandwiched between two electrodes. When high alternating current-voltage with high frequencies is applied between two electrodes, plasma is generated from the upper electrode to the lower electrode, and a wall jet-like flow is induced along the wall surface [1]. PA has some advantages for flow control such as their simple structure, no mechanical moving parts, light weight, and high responsiveness [2]. In this study, micro PA with an electrode width of the order of or less than 1mm was applied to suppress the flow separation from the NACA airfoil. Because the outline shape of the micro PA electrode could be designed freely, we adopted the wave shaped electrodes. Adjacent jets induced by the wavy electrodes collide with each other to generate streamwise vortex. Streamwise vortex mixes the momentum inside and outside the boundary layer around the airfoil and suppresses flow separation [3]. This study was used the damping type and the growing type with four rows of wavy electrodes. The electrode amplitude of the damping type PA decreases, the electrode amplitude of the growing type PA increase in the streamwise direction respectively. The both type PA were installed on the surface of a NACA63_1-012 airfoil. The effect of multi wavy type PA on flow separation suppression were investigated by flow visualization and PIV analysis.

2. Experimental Apparatus

In this study, NACA63_1-012 airfoil (the chord length c = 111 mm, the wingspan is 230 mm) was used and end plates were attached to both ends of the airfoil to ensure the two-dimensionality of the flow. The wind tunnel apparatus is a closed-circuit type wind tunnel (test section 400 mm × 400 mm). Fig. 1 shows the damping and the growing type with multiple arrays of four wavy micro-PAs. The damping type electrode shape is a sinusoidal with a wavelength of 20 mm and an amplitude of 6, 5, 4, and 3 mm which gradually decrease in the streamwise direction. On the contrary, the growing type electrode shape is a wavelength of 20 mm and an amplitude of 3, 4, 5, and 6 mm which gradually increase in the streamwise direction. Mica with a thickness of 100 µm is used as the dielectric, and it is manufactured by FISA Corporation [4]. Fig. 2 shows the experimental setup and the measured cross section for PIV visualization. The main velocity was set to 2.0 m/s, and the Reynolds number based on the chord is Re = 1.46×10^4. A micro PA is attached at a position 11 mm from the leading edge, which is 10% of the chord length. Driving voltage and frequency of the micro PA were 5 kV_{pp} (peak-to-peak) and 12 kHz. The visualization experiment is performed by the tracer particle method. The tracer particles were particles generated by a smoke generator from a mixture of water and glycol solvent. A high-speed camera (Photron SA-3) was used to visualize the x-y and y-z cross sections at 2,000 fps at around the airfoil. A 1 W laser is used as the light source. In the *x-y* section, the light was irradiated in parallel with flow, and in the y-z section, the light was irradiated in perpendicular with flow.

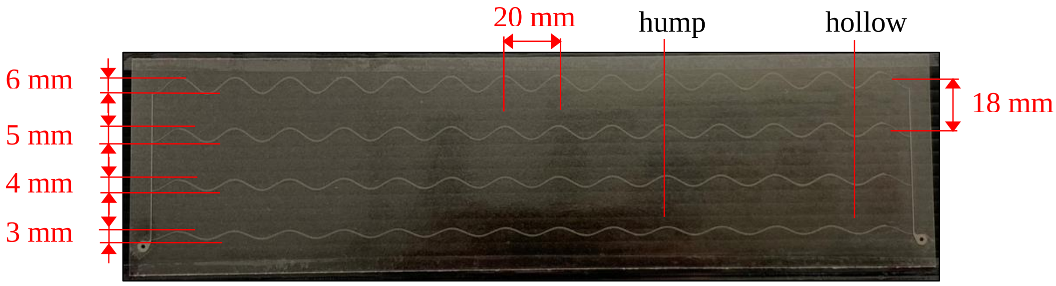

(a) Damping type

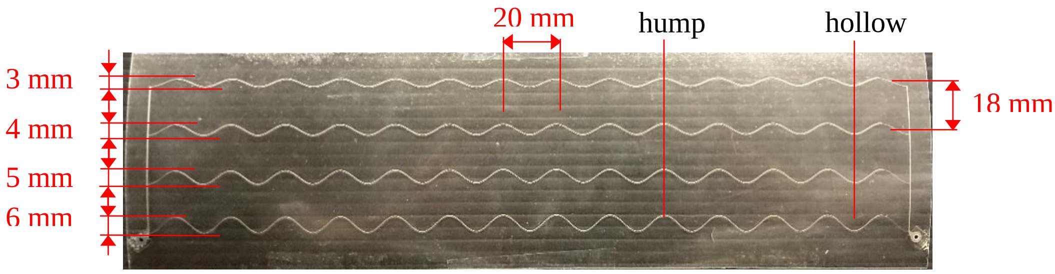

(b) Growing type

Fig. 1 Multi-Electrode wavy micro plasma actuators

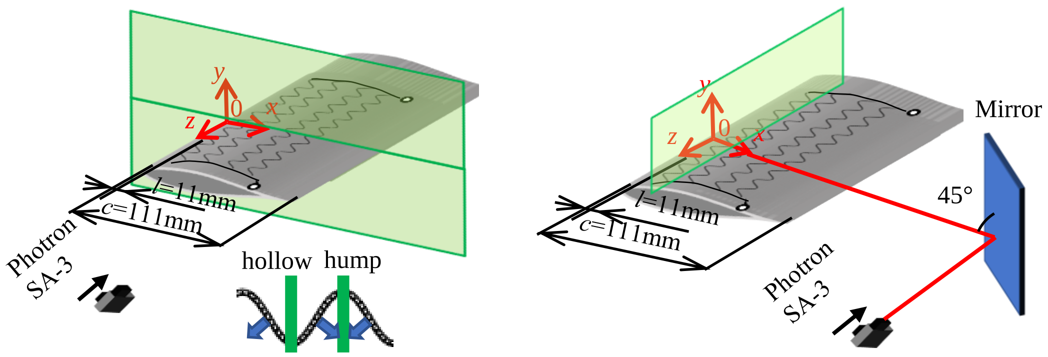

(a) x-y cross section (b) y-z cross section

Fig. 2 Experimental setup cross section for visualization

3. Experimental Results and Discussion

3.1 Flow visualization around NACA63$_1$-012 airfoil in x-y cross section

Flow visualization and PIV analysis were performed on a NACA airfoil with the damping type and the growing type at a main flow velocity of 2.0 m/s and an angle of attack of 12 deg. Fig. 3 shows the distribution of the time-mean velocity u along the x-axis direction. The red line in the figure indicates the position of the electrode, and the red circle indicates the intersection of the measuring section and the electrode. The reverse flow region on the airfoil is reduced by driving the PA in both types. Velocity profiles for each 10 % of the chord length are extracted from these results and are shown in Fig. 4. It can be seen that the PA drive suppresses flow separation for both types. In the damping type, the flow speed increases more than the growing type after the chord length of 40 %. This is because the damping type has a smaller electrode amplitude at the trailing edge of the airfoil, resulting in a larger jet in the x-axis direction on the trailing edge side of the airfoil than the growing type. It is also possible that the streamwise vortex after the chord length of 40 % induced by the growing type too small and is not enough to mix the momentum inside and outside the boundary layer. Table 1 shows the displacement thickness of both micro PAs at the chord length of 100 % and the reduction ratio by driving the PA. The reduction ratios are 66 % for the damping type and 45 % for the growing type, indicating that the damping type is more effective in suppressing flow separation than the growing type.

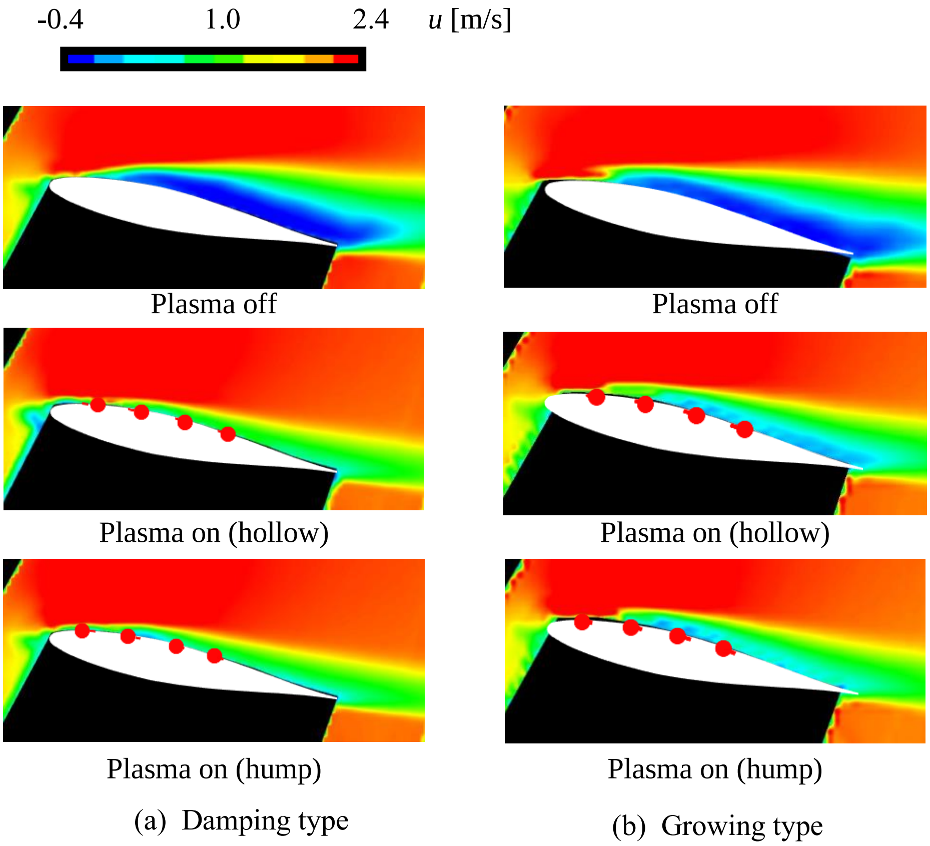

Fig. 3 Distributions of the time mean velocity

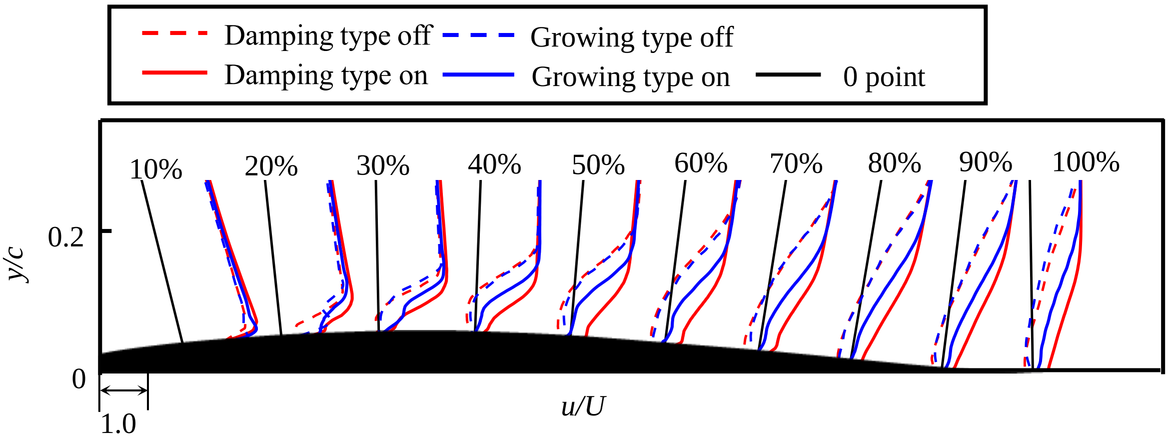

Fig. 4 Velocity profiles u in separated shear layer

Table 1 Displacement thickness

		Damping type	Growing type
Displacement thickness δ^* [mm] $\delta^* = \int_0^\infty (1 - \frac{u}{U}) dy$	Plasma off	19.0	21.0
	Plasma on	6.4	11.6
Reduction rate [%]		66	45

3.2 Flow visualization around NACA63$_1$-012 airfoil in y-z cross section

PIV analysis was performed after the 2nd and 3rd electrode row to confirm the difference in streamwise vortex caused by the PA. At the chord length of 40 % where differences began to appear in the velocity profiles. Fig. 5 and, 6 shows the distribution of the time-mean vorticity ω. The dashed lines in the figure indicate the hollow of the electrodes and the lines the hump of the electrodes. After the 2nd and the 3rd electrode row, vorticity is generated near the airfoil surface by driving the PA in both types, indicating that the PA jets delive After the 2nd and 3rd electrode row, vorticity is generated near the airfoil surface by driving the PA in both types, indicating that the PA jets have a three-dimensional flow. Periodic vortex pairs were observed on the 2nd electrode row for both micro PAs, and on the 3rd electrode row, periodic vortex pairs were observed for the growing type. The time-mean vorticity profiles at 30% of the boundary layer height when PA is not driven are shown in Fig. 7. In the 2nd electrode row, both PAs have vorticity caused by driving the PA, in the 3rd electrode row, growing type have vorticity caused by driving the PA. At the 2nd electrode row, the vorticity of the damping type is higher than that of the growing type, resulting in a periodic distribution. At the 3rd electrode row, the vorticity of the growing type is higher than that of the damping type, resulting in a periodic distribution. This indicates that the damping type induces stronger streamwise vortex in the 2nd electrode row, while the growing type induces stronger streamwise vortex in the 3rd electrode row. This is considered to be caused by the larger electrode amplitude of the damping type than the growing type in the 2nd electrode row, and the larger electrode amplitude of the growing type than the damping type in the 3rd electrode row. In addition, the magnitude of the maximum vorticity of the growing type is about 200 /s, while that of the damping type is about 300 /s, indicating that the damping type has a larger maximum vorticity than the growing type. The fact that the velocity of the damping type increases more than the growing type after the chord length of 40 % suggests that the streamwise vortex induced by the growing type after the 3rd electrode row are generated inside the boundary layer, and is not mixed the momentum. These results suggest that inducing a streamwise vortex at the leading edge of the airfoil is more effective in flow separation suppression.

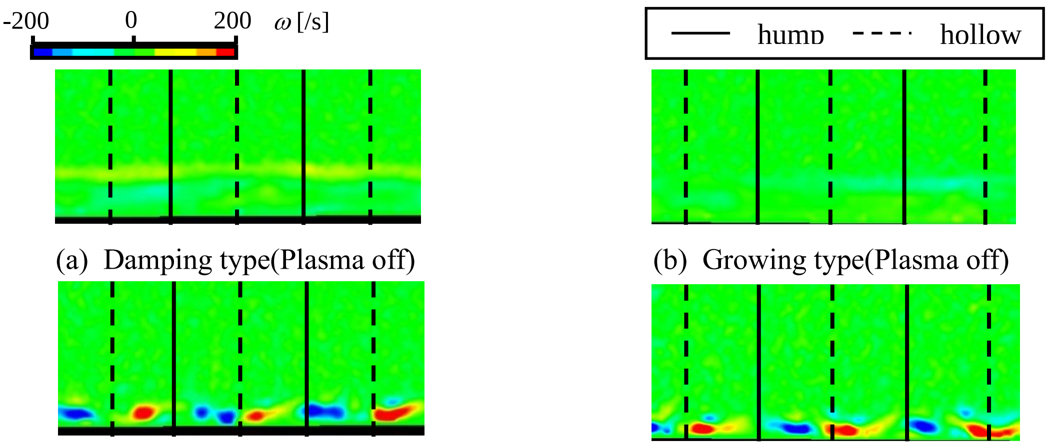

(a) Damping type(Plasma off) (b) Growing type(Plasma off)

(a) Damping type(Plasma on) (b) Growing type(Plasma on)

Fig. 5 Distributions of the time mean vorticity(after 2nd electrode)

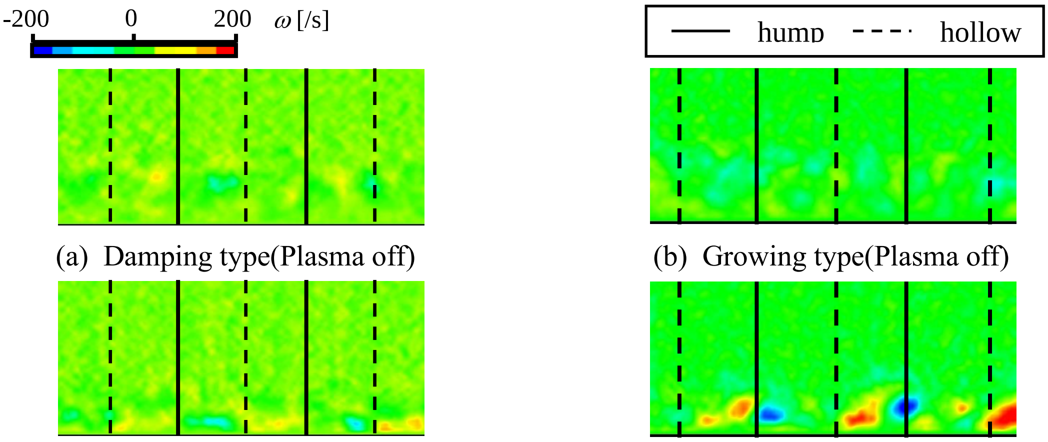

(a) Damping type(Plasma off) (b) Growing type(Plasma off)

(a) Damping type(Plasma on) (b) Growing type(Plasma on)

Fig. 6 Distributions of the time mean vorticity(after 3rd electrode)

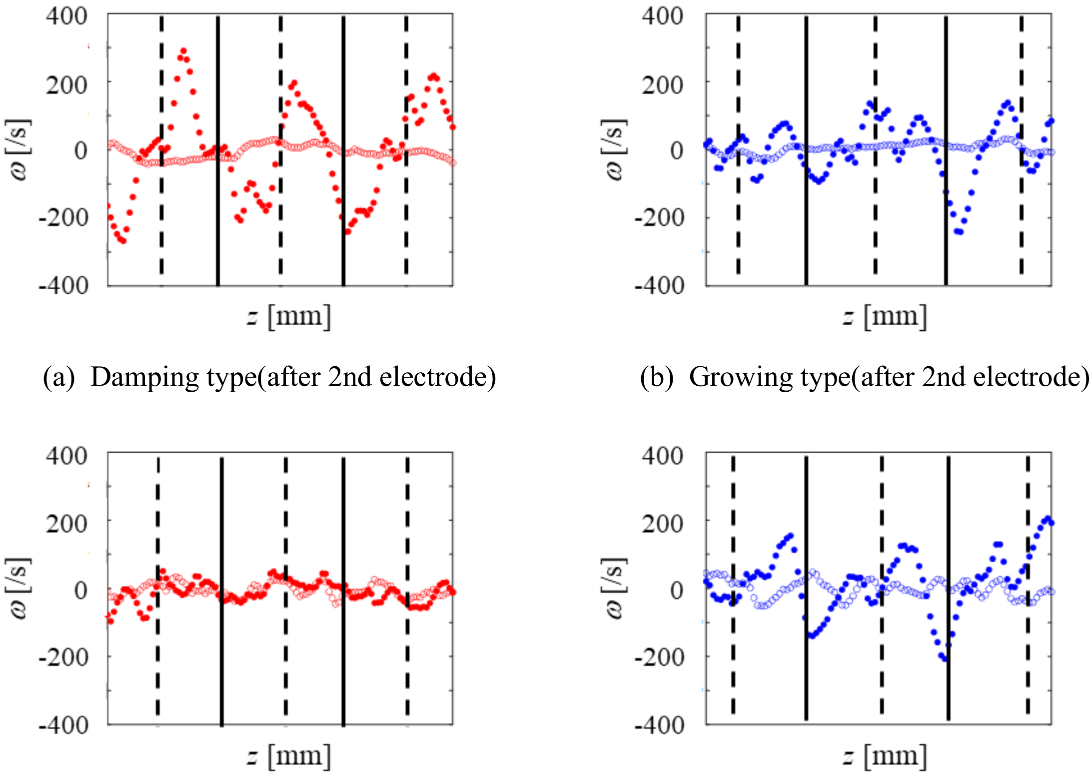

(a) Damping type(after 2nd electrode) (b) Growing type(after 2nd electrode)

(a) Damping type(after 3rd electrode) (b) Growing type(after 3rd electrode)

Fig. 7 Vorticity profiles ω (boundary layer height 30% position when PA is not driven)

4. Conclusion

As results of verifying the suppression effect on flow separation from the airfoil, by the multi-wavy micro PA, damping type and growing type, the following conclusions were obtained.

(1) In the damping type, the flow speed increases more than the growing type after the chord length of 40 % and the damping type is more effective in suppressing flow separation than the growing type.

(2) The streamwise vortex induced by the growing type after the 3rd electrode row are generated inside the boundary layer, and is not mixed the momentum.

(3) Inducing a streamwise vortex at the leading edge of the airfoil is more effective in flow separation suppression.

References

[1] Fukagata K., Yamada S. and Ishikawa H., "Plasma Actuators: Fundamentals and Research Trends", *Nagare* [in Japanese], Vol. 29, (2010), pp 243-250.

[2] Ogata S., Ikoshi Y. and Segawa T., "Control of the Jet Induced by the Plasma Actuators (Effect of the Applied Voltage Characteristics on the Jet Direction)", *Transactions of the Japan Society of Mechanical Engineers. B*, Vol.77, No.775 (2011), pp.672-679

[3] Aono, H., Yamakawa S., Iwamura K., Honami S. and Ishikawa H., "Straight and curved type micro dielectric barrier discharge plasma actuators for active flow control", *Experimental Thermal and Fluid Science*, Vol. 88(2017), pp. 16-23.

[4] FISA Corporation. https://www.fisa.co.jp/